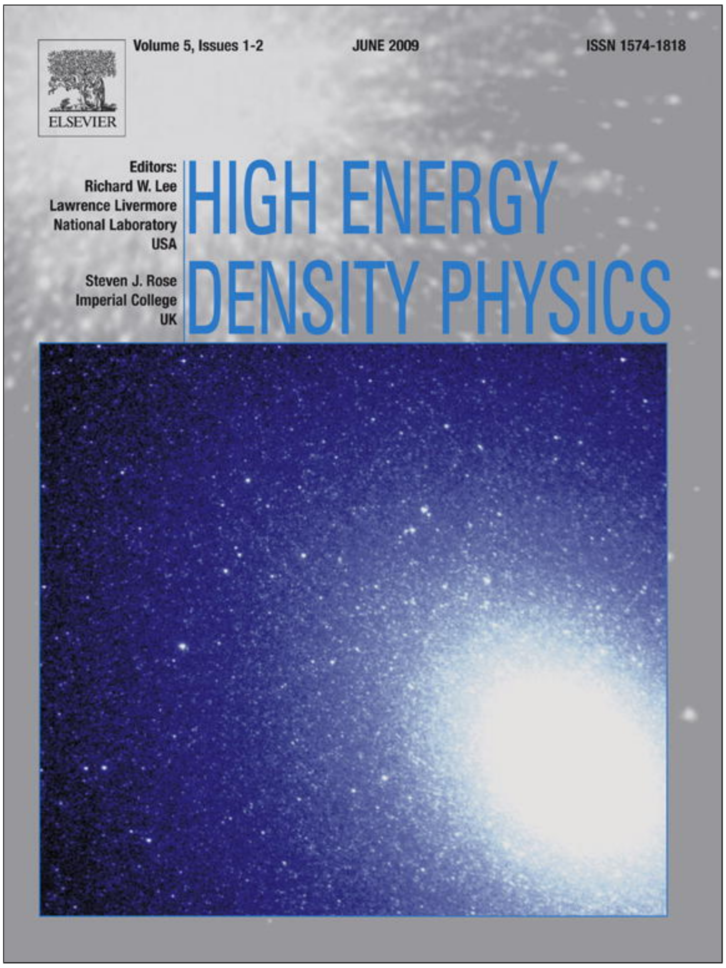
Volume 5, Issues 1-2
JUNE 2009
ISSN 1574-1818
ELSEVIER
Editors:
Richard W. Lee
Lawrence Livermore
National Laboratory
USA
Steven J. Rose
Imperial College
UK
HIGH ENERGY
DENSITY PHYSICS

High Energy Density Physics 5 (2009) 89–92

Contents lists available at ScienceDirect

High Energy Density Physics

journal homepage: www.elsevier.com/locate/hedp

Short communication

X-ray polarization splitting with the Baronova–Stepanenko spectropolarimeter

Nino R. Pereira*

Ecopulse, Inc. P.O. Box 528, Springfield, VA 22150, USA

ARTICLE INFO

Article history:
Received 2 March 2009
Accepted 2 March 2009
Available online 20 March 2009

PACS:
07.85.Nc
42.25.Ja
52.57.Kk

Keywords:
X-ray polarization
Spectroscopy
Plasma anisotropy

ABSTRACT

X-rays scattered over 90° in two mutually perpendicular directions are split into their linearly polarized components. Recently Baronova and Stepanenko realized that the three orthogonal X-ray paths are consistent with Bragg reflection over 90° when the reflecting crystal planes are under 120° with each other. These planes exist in crystals with three-fold symmetry, notably hexagonal crystals such as quartz, and in cubic crystals such as silicon and germanium. X-ray spectropolarimetry with polarization-splitting crystals can be done with various X-ray lines that are useful in diagnostics of Fast Ignition plasmas.

1. Introduction

Polarized X-ray spectra are almost always obtained by a single Bragg reflection under 45°, a technique first described [1] in the 1930s. At a 45° Bragg angle the component of X-rays linearly polarized perpendicular to the reflecting crystal plane vanishes, so that only the polarization direction parallel to the crystal plane survives. The reflecting crystal plane is usually parallel to the crystal surface, the reflection is symmetric, and the incoming and outgoing X-rays lie in a plane perpendicular to the crystal's surface. The linearly polarized component that was suppressed during the first exposure is then obtained with a second crystal rotated 90° with respect to the first, or in a second exposure with the same crystal in this second orientation.

The need for two crystals makes X-ray spectropolarimetry more difficult than X-ray spectroscopy. Experimental resources, from money to the availability of only a single line of sight to the plasma, could limit an instrument to a single crystal and a single linearly polarized spectrum. The two linearly polarized spectra needed for spectropolarimetry then demand a second exposure, from nominally the same but in fact a different plasma. Differences between the linearly polarized spectra could then come from unintended differences between the plasmas, not only from the spectrum's polarization. To a lesser degree the same problem exists even with two identical crystals: they cannot be in the same place, hence they see the plasma from different angles. When the two crystals are far enough away from the plasma, either of necessity (as in astrophysics) or when the source is strong enough and/or the registration equipment is sensitive enough, this so-called scene problem does not exist. Two carefully aligned, toroidally curved crystals, rotated 90° with respect to each other can be located far enough away that the polarized spectra come from the same plasma volume, and this work proves that plasma heating by a short-pulse laser is done in part by hot electrons with an anisotropic electron velocity distribution.

Baronova and Stepanenko [2–4] recently found an elegant way to get two linearly polarized X-ray spectra in two asymmetric Bragg reflections from a single crystal. Splitting the X-ray spectrum into its two linearly polarized components removes all ambiguity about the source of the radiation: the X-rays come in along a single path, so that both polarized spectra represent the same source (albeit averaged over the line of sight, and any other spatial or temporal averages implicit in the measurement).

Here we summarize how a single crystal splits X-rays into its two linearly polarized components as described in the literature [2–5], with some additional material that has been developed since. These analyses confirm the conclusions stated earlier, that some of the most common crystals in X-ray spectroscopy could be used also for X-ray polarization spectroscopy. Compared with the symmetric Bragg reflection geometry, a crystal rotated by 45° would split the polarization of certain other X-rays. With this information an adventurous X-ray spectroscopist could be tempted to try out X-ray polarization spectroscopy without having to obtain new

---

* Tel.: +1 703 644 8419.
E-mail address: pereira@speakeasy.net

1574-1818/$ – see front matter © 2009 Elsevier B.V. All rights reserved.
doi:10.1016/j.hedp.2009.03.005

crystals: simply turn an available crystal to its polarization-splitting geometry and supply the appropriate registration equipment.

2. Geometry for X-ray polarization splitting

The left side of Fig. 1 illustrates perpendicular scattering, the technique with which X-rays have been polarized since the early 1900s. Unpolarized X-rays come down from a point source along the z-axis. The short open blue arrow parallel to the X-axis indicates polarization in the X-direction, while the closed red arrow parallel to the Y-axis suggests polarization parallel to the Y-axis. X-rays are polarized when the incoming and scattered X-ray paths are perpendicular. Hence, X-rays scattered in the y-direction are linearly polarized along x, while X-rays scattered in the x-direction are linearly polarized along y.

When the scatterer has a regular structure, as in a crystal, the scattered X-rays can interfere constructively. This happens when the X-ray wavelength λ satisfies the Bragg condition, $\lambda = 2d \sin\theta$, with d the distance between the reflecting crystal planes. The X-rays scatter over 90° when $\theta = 45°$: for polarized X-rays the wavelength $\lambda_\perp$ is $\lambda_\perp^2 = 2d^2$.

The cubic crystal with unit length a suggested in Fig. 1 is oriented along the coordinate axes such that the crystal planes with Miller indices (011), suggested by the long dashed red lines, scatter X-rays along y. The crystal planes with Miller indices (101), the short blue dashes, scatter X-rays in the x-direction. These two planes are equivalent and have the same $2d$-spacing, so that the X-rays reflected along x satisfy the same Bragg condition as the X-rays reflected along y: these X-rays separate into their two linearly polarized components.

The two polarizing crystal planes (101) and (011) are equivalent to a third crystal plane, (110). This is the diagonal crystal plane in Fig. 1, through the Z-axis and symmetrically in between X and Y. This diagonal plane is also the mirror symmetry plane of the two polarizing crystal planes. The three crystal planes intersect along the diagonal given by the long red–blue dashes, so that they are rotated 120° with respect to each other [5]. The 120° angle between equivalent crystal planes needed for polarization splitting was first calculated [2,3] for quartz, which has hexagonal symmetry and therefore contains many polarizing planes.

Equal reflection from the two polarizing crystal planes occurs only when the X-ray geometry has the same mirror symmetry as the two planes. Therefore, the incoming X-ray path must lie in the plane of mirror symmetry, and the crystal must be cut with its surface perpendicular to the mirror symmetry plane. The right side of Fig. 1 is a side view of this plane, a rectangle with length a and $a\sqrt{2}$. The X-rays come in from the top, and in this projection lie along the rectangle's vertical edge. The two linearly polarized X-rays are both perpendicular to the incoming X-rays, so that in this projection they coincide with each other, and with the rectangle's horizontal edge as shown by the open, colored arrows marked 'full'.

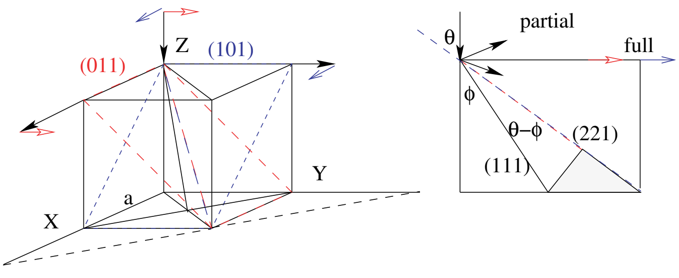

Fig. 1. (Color online) A polarizing cubic crystal.

In this projection the rectangle's top right corner is where the X-rays meet the crystal surface. Any line that goes through the top left corner can then be the projection of the crystal's surface. Crystals prefer to cleave and grow along preferred crystal planes, and crystals in X-ray spectroscopy are usually ground with their surface along specific crystal planes. The figure shows two standard choices. The (111) plane intersects the symmetry plane along line marked (111), while the line marked (221) is the cubic crystal's three-fold symmetry axis that is the diagonal of the cubic unit cell. The cubic crystals silicon or germanium are often cut along the (111) crystal plane, while the cut along the (221) plane that contains the trigonal symmetry axis is relatively rare.

A hexagonal crystal such as quartz or sapphire is often cut with its axis of hexagonal symmetry in the surface plane. The surface is then along a crystal plane with Bravais–Miller indices (hki0) (and $h + k + i = 0$). One of the most common cuts in quartz, the *C*-cut, has Bravais–Miller indices $(10\bar{1}0)$. However, the surface cut does not affect the crystal's polarizing properties provided that it is perpendicular to a mirror symmetry plane.

The angles of the incoming X-rays with the crystal's polarizing planes are, of course, fixed at 45°: how the crystal is cut determines its proper orientation with respect to the incoming X-rays. When the crystal is cut with its three-fold symmetry axis along the surface, the angle θ between the incoming X-rays and the symmetry axis was derived algebraically [4] for a hexagonal crystal, and geometrically [5] for the cubic system of Fig. 1. Briefly, in a cubic system the symmetry axis is the diagonal in the rectangle marked (221), defined by the right triangle with sides $a, a\sqrt{2}$, and $a\sqrt{3}$. Therefore, $\sin\theta = \sqrt{2/3}$ and $\theta = 54.7°$.

When the crystal is cut with its three-fold symmetry axis along the surface, the incoming X-rays also reflect from the crystal planes parallel to the surface. The angle of reflection is then θ, and the Bragg condition is $\lambda_s = 2d_s \sin\theta$ or $\lambda_s^2 = 8d_s^2/3$: the crystal planes parallel to the surface have spacing d_s. Fig. 1 shows this reflection by the short filled arrow marked 'partial'. The angle between the incoming X-ray and this reflection is $180° - 2\theta = 70.6°$: X-rays reflected from surface planes along the three-fold symmetry axis come off the crystal on the same side of the polarized X-ray reflections: their wave lengths are connected by the $2d$-spacings of the respective planes.

For a cubic crystal a more common surface cut is along the (111) crystal plane. In Fig. 1 the smaller right triangle defines the angle of the X-rays with the surface, ϕ. The triangle's edges are $a\sqrt{2}/2, a$ and $a\sqrt{3/2}$, hence $\cos\phi = \sqrt{2/3}$ and $\phi = 35.3°$: ϕ complements θ. The short unmarked filled arrow in Fig. 1 suggests this reflection that is now on the opposite side of the linearly polarized reflections, on the inside of the rectangle. For this (111) surface cut the angle of the incoming X-rays with the three-fold symmetry axis remains $\theta = 54.7°$: the three-fold symmetry axis in a cubic crystal is under an angle $\theta - \phi = 19.4°$ with the (111) plane. The shaded triangle in the mirror symmetry plane on the right side of Fig. 1 shows that $\sin(\theta - \phi) = \sqrt{1/3}$.

Fig. 2 shows a convenient way to orient a polarization-splitting crystal. The left side is for silicon, cut with its surface parallel to the (111) plane. It is mounted on the long right edge of a cylindrical block whose cross section is a right triangle with relative lengths $1, \sqrt{2}$, and $\sqrt{3}$, the same shape as in the right part of Fig. 1. X-rays parallel to the hypotenuse now have the desired angle of incidence, with $\sin\phi = \sqrt{1/3}$ or $\phi = 35.3°$. The polarizing planes inside the crystal reflect the linearly polarized X-rays, the open red and closed blue arrows, over 90° so that they overlap in this projection. The dashed arrow indicates the X-rays that reflect symmetrically from crystal planes parallel to the surface.

The right side in Fig. 2 is for a hexagonal crystal such as quartz, cut with its surface parallel to the axis of three-fold symmetry. It is

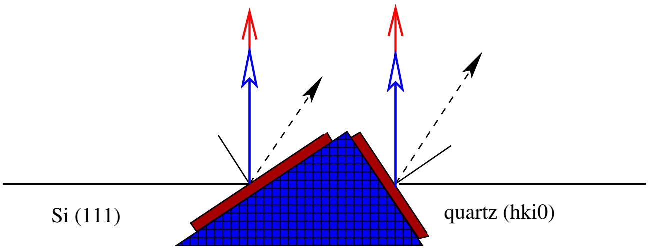

Fig. 2. Polarizing and symmetric reflections for a surface parallel to the (111) crystal plane in a cubic crystal such as silicon (left), and for a hexagonal crystal such as quartz with its three-fold symmetry axis in the surface (right).

mounted on the short edge of the rectangle, so that X-rays coming from the left have the proper angle of incidence, now with $\sin\theta = \sqrt{2/3}$ and $\theta = 54.7°$. Again, the polarized X-rays come out of the crystal perpendicular to the incoming X-rays and overlap in this projection, as illustrated by the two overlapping open red and closed blue arrows. The dashed arrow is for X-rays that reflect from crystal planes parallel to the surface.

By themselves, polarization-splitting crystals are not special: they can provide the standard, symmetric Bragg reflections that are commonly used in X-ray spectroscopy. Their special feature is that they contain crystal planes that are rotated 120° with respect to each other, which makes it possible to have three mutually perpendicular X-ray paths, incoming and two asymmetrically reflected, when the crystal is properly oriented. Perpendicular X-ray paths are a natural fit to any square or rectangular X-ray spectrometer, which would make an ideal X-ray spectropolarimeter.

Fig. 3 is the front face of the HENEX spectrometer built by NIST and NRL [6]. The red lined box in the top left behind the rectangular aperture suggests one of HENEX's four convex survey crystals. One of these crystals is quartz, cut with its surface $(10\bar{1}0)$ so that this crystal is suitable for polarization splitting [2–4]. The dashed arrow shows the symmetrically reflected X-rays from this crystal's standard orientation.

The top right aperture in Fig. 3 shows the same quartz $(10\bar{1}0)$ crystal rotated over 45°. To complete the polarizing orientation the crystal is mounted on the block of Fig. 2, this time shown perpendicular to Fig. 2. The open blue and closed red arrows suggest the two polarizing reflections rotated 90° with respect to each other, while the dashed arrow is the same symmetric reflection as in the top left.

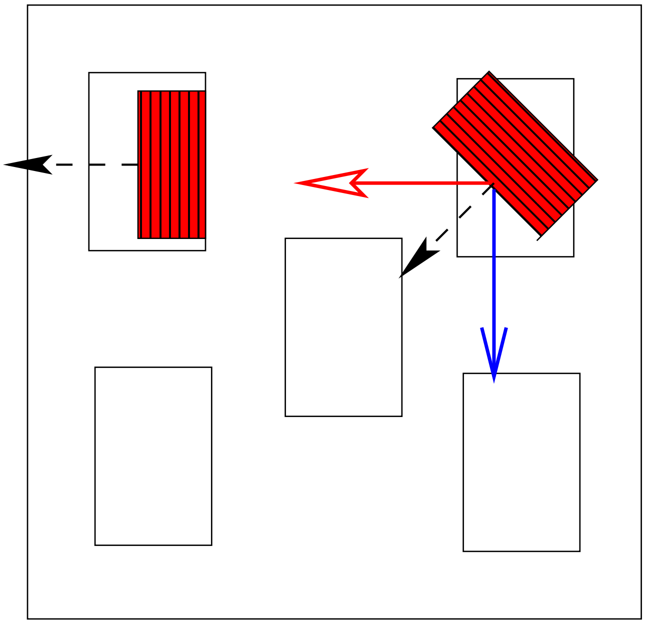

Fig. 3. Some X-ray paths in the HENEX spectrometer (top left) and a HENEX spectropolarimeter (top right).

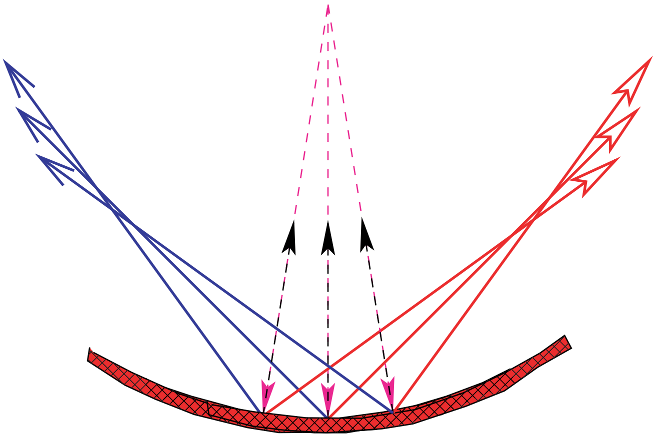

Fig. 4. Projection of the X-ray paths in a von Hamos curved crystal geometry.

X-ray spectropolarimetry with two different crystals and possibly two different X-ray emitting plasmas becomes simpler when it can be done with a single crystal that can split the X-rays into its two polarization directions. But, this simplicity comes at a cost. The crystals must be hexagonal or cubic, not all cuts work, and the crystal's axis of rotational symmetry must properly oriented with respect to the X-rays (including the plasma's anisotropy). All other issues in conventional X-ray spectroscopy remain, notably calibration, and the compromises between resolution, reflectivity, sensitivity, and throughput. Furthermore, not all the ways that these issues are dealt with in conventional X-ray spectroscopy carry over to X-ray polarization with a single crystal.

Bending the crystal changes its resolution and reflectivity, and may bring symmetrically reflected X-rays to a focus so that the intensity increases. Bending a polarization-splitting crystal changes its resolution; however, as is seen in Fig. 4 the asymmetric geometry precludes focusing of the polarized X-rays and the resulting increase in intensity.

Fig. 4 is the cross section of a cylindrically curved crystal in the von Hamos geometry, projected perpendicular to the crystal's axis of curvature. The solid magenta arrows that start in the crystal's center of curvature represent the incoming, unpolarized X-rays that reflect symmetrically, along the dashed black arrows back onto the

Table 1
Some well-polarizable photon energies in hexagonal crystals, the closest resonance ('w') X-ray line, and its Bragg angle.

Crystal	a (nm)	hki0	ε_{hkil} (keV)	Line	Angle (°)
Quartz	0.49137	$11\bar{2}0$	3.5685	K^{+17}	45.95
		$30\bar{3}0$	6.1806	Mn^{+23}	45.00
		$40\bar{3}0$	8.2409	Cu^{+27}	43.98
Sapphire	0.47628	$12\bar{3}0$	5.5235	Cr^{+22}	44.41
		$20\bar{2}0$	4.251	Sc^{+19}	44.15
Beryl	0.9088	$34\bar{7}0$	6.7757	Fe^{+24}	45.50

Table 2
Some polarizing wave lengths for (cubic, fcc) crystals Si and Ge.

Crystal	a (nm)	hkl	ε_{hkl} (keV)	Line	Angle (°)
Silicon	0.5431	404	9.1318	Zn^{+28}	45.85
Germanium	0.5660	224	6.1960	Mn^{+23}	45.14

axis of curvature, with X-rays reflecting from different axial positions on top of each other in this projection. The polarized X-rays indicated by the open blue and closed red arrows rotated 45° with respect to the incoming X-rays, in contrast, do not intersect at the same point when they reflect from different points on the crystal. Instead, they form a caustic. X-ray polarization splitting cannot use von Hamos focusing to increase the reflected X-ray intensity. However, a convex crystal that emphasizes a particular photon energy range works just as well for the symmetric as for the polarizing asymmetric reflections.

For easy reference Table 1 contains a few wave lengths and corresponding energies $\varepsilon_p = (hc/\lambda_p)/e$ for some hexagonal crystals including quartz [3] and Table 2 illustrates the same for some cubic crystals (Si and Ge). [5] These tables show only coincidences between ε_p and the spectroscopically most useful photon energy ε_Z for the resonance (‘w’) line in helium-like ions, as calculated in Ref. [7], within 1°. Many more lines become polarizable when the range is widened.

In summary we note that we treat only the hardware part of X-ray spectropolarimetry, and omit the very important problem of what can be deduced concerning the plasma from the emitted polarized X-rays. Finally, we note that a recent book by Fijimoto [8] gives a systematic introduction to X-ray spectropolarimetry.

References

[1] E. Wagner, P. Ott, Ann. der Physik 84 (1928) 425.
[2] E.O. Baronova, M.M. Stepanenko, in: Plasma Polarization Spectroscopy Workshop, P. Beiersdorfer, 2001.
[3] E.O. Baronova, M.M. Stepanenko, Plasma Phys. Control. Fusion 45 (2003) 1113.
[4] E.O. Baronova, M.M. Stepanenko, A.M. Stepanenko, Rev. Sci. Instrum. 79 (2008) 083105.
[5] N.R. Pereira, J. Mod. Optic. 5 (2007) 2563.
[6] L.T. Hudson, R. Atkin, C.A. Back, A. Henins, G.E. Holland, J.F. Seely, C.I. Szabo, Radiat. Phys. Chem. 75 (2006) 1784.
[7] A.N. Artemyev, V.M. Shabaev, V.A. Yerokhin, G. Plunien, G. Soff, Phys. Rev. A 71 (2005) 062104.
[8] T. Fujimoto, A. Iwamae, Plasma Polarization Spectroscopy, Springer, 2007.